

Pharmacological DNA Demethylation Weakens Inhibitory Synapses in the Auditory Cortex and Re-Opens the Critical Period for Frequency Map Plasticity

Benjamin A. Schwartz¹, Weihua Wang², Shaowen Bao^{1,2,*}

¹Neuroscience Program and ²Departments of Physiology, University of Arizona, Tucson, AZ 85724.

Running title: Epigenetic Modulation of Critical Period

* Correspondence to: Shaowen Bao, Ph.D. (sbao@email.arizona.edu)

Abstract

The critical period is a time of maximal plasticity within the cortex. The progression of the critical period is marked by experience-dependent transcriptional alterations in cortical neurons, which in turn shifts the excitatory-inhibitory balance in the brain, and accordingly reduces plasticity. Epigenetic mechanisms, such as DNA methylation, control the transcriptional state of neurons, and have been shown to be dynamically regulated during the critical period. Here we show that adult animals have a significantly higher concentration of DNA methylation than critical period animals. Pharmacological reduction of DNA methylation in adult animals re-establishes critical period auditory map plasticity. Furthermore, the reduction of DNA methylation in adult animals, reverted intrinsic characteristics of inhibitory synapses to an immature state. Our data suggest that accumulation of DNA methylation during the critical period confers a mature phenotype to cortical neurons, which in turn, facilitates the reduction in plasticity seen after the critical period.

Keywords: Epigenetics; Critical Period; DNA Methylation; Plasticity

Introduction

The critical period (CP) is a developmental epoch of heightened cortical plasticity (Hensch, 2005). Throughout the CP, experience drives the wiring of cortical circuits that refines sensory maps and motor maps (O'Leary, 1994; Katz and Crowley, 2002; Villers-Sidani, 2007). Once the CP is closed, plasticity within the sensory cortex decreases considerably, and requires additional neuromodulatory mechanisms for induction (Keuroghlian and Knudsen, 2007). Elucidating the mechanisms that facilitate plasticity during the CP and the mechanisms that restrict plasticity in adulthood, is vital for understanding how plasticity is regulated in the brain.

The progression of the CP is marked by experience-dependent maturation of inhibitory neurons (Hensch, 1998; Dunning et al., 1999; Huang, 1999; Fagiolini, 2000; Itami et al., 2007), and a shift in the transcriptional profile of these cells (Majdan and Shatz, 2006; Okaty et al., 2009). Recently, studies have begun to probe the contribution of DNA methylation (DNA-ME) to CP dynamics. Sequencing experiments have shown during early development frontal cortical and dentate granule neurons rapidly accumulate DNA-ME that persists into adulthood (Lister et al., 2013; Guo et al., 2014). Overexpression of GADD45b, a protein involved in activity-dependent DNA demethylation, reopened ocular dominance plasticity in adult mice, suggesting that DNA demethylation enhances plasticity (Apulei et al., 2019). However, inhibition of DNA-ME during the CP via RG108 blocked ocular dominance plasticity, suggesting a facilitating role of DNA-ME on plasticity (Tognini et al., 2015). Conditional knockout of MeCP2 (a methyl-binding protein and one of the primary effectors of DNA-ME) in parvalbumin positive interneurons also blocked ocular dominance plasticity in the critical period (He et al., 2014). These results suggest that DNA

methylation plays a crucial role in postnatal development, but more research is required to understand its role in regulating critical period plasticity.

In this study, we measured global levels of DNA-ME in the auditory cortex of adult and CP mice using a quantitative colorimetric ELISA. Adult mice had significantly higher levels of DNA-ME compared to CP mice. Pharmacological DNA demethylation of adult mice, via 5-aza2'-deoxycytidine (5-aza) injections, re-opened CP auditory map plasticity in adult mice, while vehicle injections did not. Global DNA demethylation in adult mice decreased the frequency and increased the decay time constant of miniature inhibitory synaptic currents (mIPSC's) onto pyramidal cells, indicating a shift towards an immature state of inhibitory synapses that is seen during the CP. RT-PCR experiments revealed that BDNF and REST, two genes that are developmentally regulated, and heavily implicated in the maturation of the cortex (Hanover et al., 1999; Huang, 1999; Ballas et al., 2005; Rodenas-Ruano et al., 2012) reverse their transcription levels back to critical period levels. Overall, these results suggest that global levels of DNA-ME influence the maturation of cortex and reducing global levels of DNA-ME can re-open the critical period by reversing characteristics of cortical maturation.

Methods

Animals:

All procedures in this study were approved by the Animal Care and Use committee at the University of Arizona. WT (FVB.129P2-Pde6b⁺Tyr^{c-ch}/AntJ) mice were originally obtained from The Jackson Laboratory. Both females and males were used in these experiments. A total of 64 mice were used for this experiment.

Sound Exposure:

Sound exposure was performed as previously described (Zhang et al., 2001). Litters of 2 to 5 mice were placed in a ventilated, sound-shielded, calibrated test chamber for 7-14 days (depending on the experiment) and exposed to 16 kHz pure tone pips, or tone pips spanning 2kHz-48kHz (acoustic enrichment). A 25-ms tone (5-ms ramps) at 60–70 dB SPL was applied from a speaker placed about 15 cm above the mice, at 6 pulses per second with 1-s intervals to minimize adaptation effects. No noticeable distortion of tonal stimuli was detected from sound spectrum recorded inside the test chamber. There were no significant spectral peaks for the normal environmental noise background. The total sound pressure level in the animal room was 5–10 dB lower than that of exposed tonal stimulus intensity. Inside the sound attenuation chamber with the presence of mice, but in the absence of the tone stimulus, the noise level was about 15–25 dB below that in the animal room at all frequencies within the mouse's hearing spectrum. No significant harmonic signal was found in the chamber when a tonal stimulus was being delivered.

Pharmacological injections:

Pharmacological inhibition of DNA methyltransferase was achieved using 5-aza2'-deoxycytidine (Chabot et al., 1983; Sales et al., 2011). Adult mice between p60-p120 were injected intraperitoneally with either 2 mg/kg of 5-aza (mixed with DMSO and filtered 1X PBS) or a vehicle injection of just DMSO and filtered 1X PBS. These injections were repeated for 7 days, at approximately the same time every day.

Electrophysiological recording procedure: The primary auditory cortex (AI) of mice was mapped as previously described (Kim et al., 2013), except as follows. Mice were anesthetized with ketamine (100 mg/kg, i.p.) and xylazine (10 mg/kg, i.p.), and kept anesthetized with, a steady flow of 1% isoflurane. The cortex was maintained under a layer of silicone oil, that was reapplied as necessary. Multiunit responses to 25 ms pure tone pips (2–74 or 4 –74 kHz, 0.1 octave increments at 0–70 dB, 10 dB increments) were recorded using tungsten microelectrodes (FHC) in the thalamorecipient layer of AI (350 – 450 micrometers below the cortical surface). References to neurons in this text refer to multiunit responses recorded extracellularly. Tones were presented to the left ear through an electrostatic speaker (Tucker Davis Technologies) at 3 pips per second and each frequency-intensity combination was repeated three times. Cortical penetration locations were recorded on a high-resolution image, which was later used to construct the map.

AI mapping analysis:

Receptive fields and response properties were isolated using custom-made programs in MATLAB as previously described (Insanally et al., 2010), except as follows. The peak of the peristimulus time histogram (PSTH) within a window from 7 to 50 ms after the stimulus onset was defined as the response latency. The response window was defined as a period encompassing the PSTH peak, in which the firing rate was higher than the baseline firing rate. The spikes in the response window were counted to reconstruct the receptive field. The map of AI was generated using the voroni tessellation algorithm, in which the characteristic frequency (CF) of the receptive field is converted to a polygon of a certain area. The area of the polygons dedicated to a CF of 16 kHz (+/- .2 octaves) were summed and then divided by the total area to determine the percent of AI dedicated to 16 kHz. For comparing the ratio of area dedicated to 16kHz, to low frequency, the area of the polygons dedicated to 9.2 kHz and 12.1 kHz (+/- .2 octaves) were summed. We then

divided the area dedicated to 16 kHz by the summation of the area dedicated to the two low frequency bins.

AI dissections/DNA extractions/DNA methylation quantification:

Mice were anesthetized with ketamine (100 mg/kg, i.p.) and xylazine (10 mg/kg, i.p.). Mice were then perfused with cold 1X PBS for 10 minutes. Following perfusion, mice were decapitated, and their brains harvested. In a dish filled with cold 1X PBS, the brain was cut just in front of the inferior colliculus, and just behind the region where the two hemispheres connect. The auditory cortex, which is 1 mm above the rhinal fissure, was subsequently dissected from both hemispheres. DNA from these tissue samples were then extracted using the QIAamp Fast DNA Tissue kit. Final DNA concentrations were then measured using a nanodrop. The samples of extracted DNA were then subjected to the MethylFlash Methylated DNA 5-mC Quantification kit for quantification of DNA-ME. This kit utilizes a colorimetric assay with an antibody specific to 5-mC to measure global levels of DNA-ME.

Patch Clamp:

Patch clamp electrophysiology was conducted on mice that were injected with 5-aza or treated as different conditions exposure as described below ($n \geq 4$ mice for each group). The brain was extracted and immediately placed in an oxygenated (95% O₂/5% CO₂) external solution (87 mM NaCl, 2.5 mM KCl, 7 mM MgCl₂, 25 mM D-glucose, 25 mM NaHCO₃, 1.25 mM NaH₂PO₄, 0.5 mM CaCl₂, and 75 mM Sucrose at pH 7.3). The brain was sectioned along the transverse plane into 300 μ m slices with a vibrating microtome (Leica; VT1000S), and brain slices were immersed in oxygenated external solution in a tissue chamber for 30 min at 32.5°C. Then slices were allowed to acclimate to room temperature for at least 30 min before recording. The recording chamber was

continuously perfused with oxygenated artificial cerebrospinal fluid (aCSF) (125 mM NaCl, 2.5 mM KCl, 1 mM MgCl₂, 25 mM D-glucose, 25 mM NaHCO₃, 1.25 mM NaH₂PO₄ and 2 mM CaCl₂ at pH 7.3) at a rate of 2 mL/min and maintained at 32°C. A fixed stage microscope (Olympus; BX51WI) equipped with differential interference contrast optics and a 40× water-immersion objective was used to visualize individual neurons in the AI.

Patch electrodes had an impedance of 3–5 MΩ when back-filled with the internal solutions for miniature inhibitory postsynaptic currents (mIPSCs) measurement (135 mM CsMs, 10 mM CsCl, 10 mM Hepes, 0.2 mM EGTA, 4 mM ATP-Mg, 0.4 mM GTP-Na at pH 7.3 and 290 mOsm). The initial access resistance typically ranged from 15 to 23 MΩ and remained stable during the recording session. Series resistance was also continuously monitored with a brief voltage pulse. Recordings were accepted when a cell had a series resistance of 15–25 MΩ (<20% change during the recording session). mIPSCs were recorded in oxygenated aCSF solution containing 1 μM Tetrodotoxin (TTX), 20 μM 6-Cyano-7-nitroquinoxaline-2,3-dione (CNQX), and 100 μM D-2-amino-5-phosphonovalerate (DAP5). Cells were held at 0 mV throughout the experiment. Signals were low pass filtered at 2kHz. Experiments were conducted using Axon Instruments hardware and software (MultiClamp 700B, Digidata 1550A, pClamp 10.5). 0.3% biocytin was added into the internal solution before recording to identify the morphology of pyramidal cells. After recording, data were collected and analyzed with pCLAMP software (Molecular Devices) and MiniAnalysis (Synaptosoft). Slices were prepared from four or more mice for each group, and only one neuron was recorded from each slice. Data analysis shown for both individual neurons as well as the averages per animal in each experimental group.

Quantitative real-time PCR

The harvesting of AI tissue was accomplished in the same way described in the “AI dissections/DNA extractions/DNA methylation quantification” section. The only difference is the tissue samples were stored in an RNA stabilizing reagent, RNA *later* (Qiagen). RNA was extracted from the tissue using the Quick-RNA mini prep kit (Zymo Research). Immediately following extraction, the total RNA concentration and A260:A280 ratio of each sample were determined via NanoDrop 2000 (Thermo Scientific). The High Capacity cDNA Reverse Transcription kit (Thermo Fischer) was used to generate cDNA in a thermal cycler (ABI9700) for 2 hours at 37°C. Ten nanograms of cDNA were used in each reaction for real-time PCR using the CFX96 Real-Time PCR system (Bio-Rad Laboratories, Hercules, CA). Threshold cycle (Ct) values of the target genes were normalized to the endogenous control gene (GAPDH). The primer sequences are as follows: GAPDH; Forward- ACCTTTGATGCTGGGGCTGGC, Reverse- GGGCTGAGTTGGGATGGGGACT, BDNF; Forward-CAGGAGTACATATCGGCCACCA, Reverse- GTAGGCCAAGTTGCCTTGTCCT, REST; Forward- CATGGCCTTAACCAACGACAT, Reverse- CGACCAGGTAATCGCAGCAG.

Statistical analysis

Statistical analyses were conducted using SPSS software. When comparing two groups, independent samples t-test was used, unless the distribution wasn't normal, in which case a Mann-Whitney U test was used. Group comparisons of variables were made using a one-way analysis of variance (ANOVA) followed by a *post hoc* least significant difference (LSD) test, unless the data was not homoscedastic, in which case a Kruskal-Wallis H test followed by a *post hoc* Dunn Test with Bonferonni correction for multiple comparisons was performed. Homogeneity of variance

was tested using Levene's test (based on median), and normality was tested using the Kolmogorov-Smirnov test with Lilliefors Significance Correction. A $p < 0.05$ was considered statistically significant.

Results

Reducing global levels of DNA-ME re-establishes auditory critical period map plasticity

Recent evidence suggests that frontal cortical and dentate granule neurons accumulate DNA-ME over the course of development (Lister et al., 2013; Guo et al., 2014). To confirm that this phenomena also occurs in sensory cortex, we performed a colorimetric ELISA to measure global levels of DNA-ME in the auditory cortex of adult mice, and mice in the CP. Adult mice between the ages of 2-4 months (n=12), and CP mice (n = 6) at post-natal (PN) day 11 were sacrificed, and their brains harvested for DNA-ME analysis. An independent samples t-test showed that the auditory cortices of adult mice had a significantly higher concentration of DNA-ME than auditory cortices of CP mice ($t_{11.53}=2.97$, degrees of freedom adjusted due to unequal variance, $p = 0.012$; Figure 2A). These results indicate that along with frontal cortical and subcortical structures, neurons within sensory cortex also accumulate DNA-ME over the course of development.

These results led us to hypothesize that if neurons in the auditory cortex accumulate DNA-ME over the course of development, then reducing the global DNA-ME levels may return adult cortex to a more plastic state as is seen in the critical period. To test this hypothesis, we probed the level of plasticity in the AI frequency map of five different experimental groups (Figure 1). The first group were Naïve mice that received no injections nor exposure (Naïve; n = 5). The second group were CP mice exposed to 16 kHz tone pips from PN9 until the day of A1 mapping (PN19-PN23) (CP-expo; n = 5). The third group were adult mice between the ages of 2-4 months that received 7 days of 5-aza injections concurrently with 10-14 days of 16 kHz exposure (Dem-expo; n = 5). The fourth group was a group of adult mice injected with vehicle and concurrently exposed

to 16 kHz for 10-14 days (Veh-expo; n = 5). Finally, the fifth group was a group that received 7 days of 5-aza injections without exposure, and were subsequently mapped the day after the final injection (Dem; n = 4). Compared to the Naïve group, both CP-expo and Dem-expo groups showed a significant increase in the average area in AI dedicated to the exposure frequency of 16 kHz, (ANOVA: $F_{4,19}=20.36$, $p < 0.0005$; *post hoc* LSD: $p < 0.0005$ for both groups, Figure 2B). The Veh-expo group, as well as the Dem group, did not show such an increase in the representation of the exposed frequency (*post hoc* LSD: $p = 0.264$, and $p = 0.922$ respectively). This indicates that neither demethylation, nor sound exposure alone was sufficient to induce a significant expansion in the 16 kHz frequency band of AI in adult mice. We also analyzed the ratio of the area dedicated to 16 kHz to the area dedicated to a low frequency bin (from 8 kHz to 13.91 kHz), in the five experimental groups. The CP-expo and Dem-expo groups showed an increase in the 16 kHz to low frequency area ratio relative to Naïve (Figure 2C; ANOVA: $F_{4,19}=10.90$, $p < 0.0005$; *post hoc* LSD $p < 0.0005$, and $p=0.002$ respectively). No increase was seen in the 16 kHz to low frequency area ratio for either the Veh-expo nor Dem mice, relative to Naïve mice (*post hoc* LSD: $p = 0.544$, and $p = 0.729$ respectively). To verify that 5-aza was in fact reducing global methylation levels, we performed another colorimetric ELISA on auditory cortex samples from 5-aza treated mice (n=4) and vehicle treated mice (n=8). Results from the ELISA confirmed that 5-aza treatment facilitated global demethylation. (Figure 2D; Mann-Whitney U test: $U_{8,4}=2.0$, $p = 0.016$). These results indicate that reducing DNA-ME in adult mice can re-establish auditory frequency map plasticity similar to that observed in the critical period.

As previously mentioned, DNA demethylation via overexpression of GADD45b, was sufficient to re-open the critical period for ocular dominance plasticity within primary visual cortex

(Apulei et al., 2019). That study also showed that overexpression of GADD45b led to a significant decrease in overall sensory response strength in both eyes. Therefore, we analyzed the average threshold for receptive fields collected from the five experimental groups, to determine whether pharmacological DNA demethylation also induced a general depression in sensory response. The CP-expo mice had a significantly lower average threshold for auditory evoked signal in AI, relative to the other experimental groups (Figure 3A; ANOVA; $F_{4,19} = 10.52$, $p < 0.0005$; *post hoc* LSD: $p < 0.0005$ [CP-expo compared to Naïve]). Treatment with 5-aza did not significantly alter average threshold relative to the Naïve group for either the dem nor dem-expo group (*post hoc* LSD: $p = 0.139$ and $p = 0.813$, respectively). We also analyzed the average response amplitude between the five groups, and found an overall significant difference between the groups (data not shown: Kruskal-Wallis H Test; $H_4=10.1$, $p < 0.039$). *Post hoc* analysis showed a significant increase in response amplitude for the CP-expo relative to the Naïve group (group means: CP-expo= 10.26 spikes/tone, Naïve = 7.77 spikes/tone; *post hoc* Dunn Test: $p = 0.015$), but there were no significant differences between the Naïve group and the other experimental groups (*post hoc* Dunn Test: $p > 0.05$ for all other groups relative to Naïve). Other receptive field features, such as response latencies, have been shown to change over the course of the critical period. Response latencies decrease most dramatically during the critical period, but continue to decrease through P60 (Villers-Sidani, 2007). We analyzed response latencies in the five experimental groups and found overall significant differences in onset, peak and offset of the auditory response. (onset, Figure 3B: ANOVA; $F_{4,19}=7.79$, $p = 0.001$; peak, Figure 3C: ANOVA; $F_{4,19}=4.86$, $p = 0.007$; offset, Figure 3D: ANOVA; $F_{4,19}= 4.89$, $p =0.007$). More specifically, the CP-expo and the Dem group had significantly longer onset (*post hoc* LSD: $p = 0.001$, and $p =0.011$, respectively), peak (*post hoc* LSD: $p = 0.018$, and $p =0.004$, respectively), and offset (*post hoc* LSD: $p = 0.018$, and $p =0.004$,

respectively), relative to the Naïve group. This indicates that 5-aza treatment results in longer response latencies as seen during development (Villers-Sidani, 2007).

Reducing global DNA-ME reverts inhibitory synaptic function to an immature state

As maturation of cortical inhibition is shown to parallel the critical period, we hypothesized that global DNA demethylation is affecting inhibitory synaptic transmission in the auditory cortex. To test this hypothesis, we recorded mIPSCs from pyramidal neurons in Layers 2/3 of AI (Figure 4A,B). We used the same experimental groups, with the only difference being that we changed the exposure stimulus from solely 16 kHz tone pips, to tone pips ranging from 2-48 kHz, to assure that all of the frequency sensitive neurons within AI were receiving auditory input during the treatment period. The frequency of mIPSCs (Figure 4C) steadily increased over four days of the CP (PN11-PN14). The overall average frequency of mIPSC's during the CP was less than half the average frequency seen in Naïve adult mice and Veh-expo adult mice. One-way ANOVA revealed a significant main effect (ANOVA on individual neurons: $F_{4,74} = 20.57$, $p < 0.001$; ANOVA on animal average: $F_{4,15} = 7.628$, $p = 0.001$) and *post hoc* analysis showed a significant difference between the CP and Naïve adult groups (*post hoc* LSD: neurons: $p < 0.001$; animals: $p < 0.001$) and between CP and Veh-expo adult groups (*post hoc* LSD: neurons: $p < 0.001$; animals: $p = 0.001$). The mIPSC frequency significantly decreased in the Dem group compared to the Naïve group (*post hoc* LSD: neurons: $p < 0.001$; animals: $p = 0.017$). Dem-exp and Naïve were different only when data from individual neurons were compared (*post hoc* LSD: neurons: $p = 0.035$; animals: $p = 0.361$). When analyzing the amplitude of mIPSC's (Figure 4D), we saw an increase in amplitude over the course of the CP which is expected because this is a time marked by significant synaptogenesis. However, we saw no overall difference across the five experimental groups in terms of mIPSC amplitude

(ANOVA on neurons: $F_{4,74} = 2.41$, $p = 0.068$; ANOVA on animals: $F_{4,15} = 2.473$, $p = 0.089$). Finally, we analyzed the mIPSC decay time constant (Figure 4E), which has been shown to decrease as cortical neurons develop (Dunning et al. 1999). Our results confirmed that mIPSC decay time constant decreases from early post-natal life to adulthood. One-way ANOVA revealed a significant main effect (ANOVA on neurons: $F_{4,76}=7.92$, $p = 0.001$; ANOVA on animal mean: $F_{4,15} = 7.92$, $p = 0.004$) and *post hoc* analysis showed significant differences in between the CP group and both the Naïve adult and Veh-expo group adulthood (*post hoc* LSD: comparing neurons: $p = 0.006$ between CP and Naïve, $p < 0.001$ between CP vs. Veh-expo; comparing animals: $p = 0.048$ between CP and Naïve, $p < 0.001$ between CP and Veh-expo; Figure 2E). By contrast, the mIPSC decay time constant was not different between the CP group and the two DNA-demethylated groups (*post hoc* LSD: comparing neurons: $p = 0.059$ between CP and Dem-expo, $p = 0.118$ between CP and Dem,). Global DNA demethylation in exposed and unexposed mice significantly increased the mIPSC decay time constant relative to Veh-expo adult mice (*post hoc* LSD: comparing neurons: $p = 0.025$ between Dem-expo and Veh-expo, $p = 0.005$ between Dem vs. Veh-expo; comparing animals: $p = 0.015$ between Dem-expo and Veh-expo, $p = 0.004$ between Dem and Veh-expo). Overall, these results indicate that reducing global levels of DNA-ME shifts certain aspects of the cortical inhibitory synapse to an immature state similar to that observed in the critical period.

Reducing global DNA-ME reverses expression of developmentally regulated genes to CP levels

The results from the patch clamp experiments revealed that upon treatment with 5-aza, specific characteristics of mature inhibitory synaptic function were reversing to an immature state. These results led us to hypothesize that genes that participate in the maturation of the cortex may

also be reverting back to levels seen during the CP upon treatment with 5-aza. To address this, we investigated the expression levels of two genes that are implicated in cortical maturation during the CP, BDNF exon IV (Hanover et al., 1999; Huang, 1999; Hensch, 2005), and REST (Ballas et al., 2005; Rodenas-Ruano et al., 2012), via RT-PCR. Our results confirmed that both of these genes are developmentally regulated in that BDNF exon IV expression was significantly lower in CP mice compared to adult Naïve mice (Figure 5A; ANOVA: $F_{4,18} = 4.62$, $p = 0.01$, *post hoc* LSD: $p = 0.004$), and REST expression was significantly higher in CP mice compared to adult Naïve mice (Figure 5B; ANOVA: $F_{4,19} = 3.05$, $p = 0.042$, *post hoc* LSD: $p = 0.012$). Seven days of 5-aza treatment was sufficient to induce a significant reduction in BDNF exon IV expression (*post hoc* LSD: $p < 0.05$ for both demethylated groups). Mice treated with vehicle for seven days did not see a significant change in BDNF exon IV expression relative to Naïve mice (*post hoc* LSD: $p > 0.05$). In terms of REST expression, neither 5-aza treatment, nor environmental enrichment alone were sufficient to significantly increase REST expression relative to Naïve mice. However, the combination of environmental enrichment and 5-aza treatment significantly increased REST expression levels relative to Naïve mice (*post hoc* LSD: $p < 0.020$). The magnitude of this change was similar to the expression levels seen during the CP. These data suggests that global DNA demethylation facilitates the reversal of expression of genes implicated in cortical maturation and plasticity to levels seen during the CP.

Discussion

The main finding of this study is that pharmacological DNA demethylation in adult mice enables sound exposure-induced frequency map reorganization, which is typically observed only

in the critical period but not in adulthood. This elevated cortical plasticity is accompanied by an increase in the response latencies, a reduction in mIPSC frequency and an increase in mIPSC decay time constant to levels that are normally observed during development. Furthermore, DNA demethylation in adult mice also reversed BDNF and REST expression to levels similar to those in critical period. These concerted changes suggest that global demethylation reopens the critical period for frequency map plasticity in the auditory cortex. These results are consistent with the findings that overexpression of GADD45b, a protein involved in DNA demethylation, reopened ocular dominance plasticity in adult visual cortex (Apulei et al., 2019). Considering the differences between inducing auditory map plasticity, and ocular dominance plasticity, as well as the inherent differences between the auditory and visual cortex, we find this confluence of results to be interesting, and suggests that DNA-ME acts as a universal mechanism for regulating plastic states within sensory cortex. Together with reports that histone acetylation modulates ocular dominance plasticity, these results highlight epigenetic modulations as an important contributor to neural plasticity during development and in adulthood (Putignano et al., 2007; Gervain et al., 2013; Baroncelli et al., 2016). However, not all of our findings are consistent with the GADD45b overexpression study. In that study, the authors found a general reduction in visual responses as a result of GADD45b overexpression. Treatment with 5-aza did not lead to a similar reduction in auditory response. The difference in these results could be explained by the different demethylation method. Studies have shown that inhibiting DNA methyltransferases can yield different synaptic effects than over-expressing proteins that catalyze active DNA demethylation (Yu et al., 2015; Sweatt, 2016). More studies are required to better understand how the downstream pathways of inhibiting DNA-ME or strengthening DNA demethylation can yield differing effects on synaptic transmission.

DNA demethylation has been shown to upscale excitatory glutamatergic synapses, and enhance intrinsic membrane excitability in cultured cortical neurons (Meadows et al., 2015; Meadows et al., 2016). To our knowledge, our results are the first to show that DNA demethylation also downregulates cortical inhibitory synapses by decreasing mIPSC frequency. This is consistent with the observed reduction of BDNF expression, as BDNF has been shown to upregulate GAD65 expression, increase mIPSC frequency, promote maturation of inhibitory neurons and inhibit ocular dominance shift by monocular deprivation (Hanover et al., 1999; Huang, 1999; Bolton et al., 2000; Galuske et al., 2000; Maffei, 2002; Ohba et al., 2005). As developmental maturation of cortical inhibitory circuit is an important regulator of the critical period (Hanover et al., 1999; Huang, 1999; Hensch, 2005), the observed reversal of inhibitory synaptic properties likely contributed to the reopening of the critical period for frequency map plasticity following DNA demethylation. We also found that DNA demethylation prolongs response latencies to levels seen during the CP. Interestingly, a similar result was found in a transgenic model of MeCP2 duplication syndrome. Transgenic overexpression of MeCP2 led to significantly prolonged response onset and response peak in the AI of the transgenic mice, relative to wild-type control (Zhou et al., 2019). These findings establish a potentially important connection between DNA-ME dynamics and auditory response latencies in the cortex.

The gene expression patterns observed after 5'aza treatment are consistent with reduced inhibitory synaptic transmission observed in this study. For example, 5'aza treatment reduced BDNF expression in our study, which, at first glance, was surprising because increased BDNF expression has been implicated in heightened plasticity levels (West et al., 2001; Lu et al., 2008),

and because other studies have shown that DNA-ME negatively regulates BDNF expression (Martinowich et al., 2003). However, increased BDNF is also heavily implicated in promoting maturation of cortical interneurons during the CP (Hanover et al., 1999; Huang, 1999), correlating with potentiated inhibition levels (Maffei, 2002) and subsequently reduced plasticity. Furthermore, it has been shown that direct BDNF infusions into adult cat visual cortex did not influence orientation selectivity or ocular dominance, suggesting that increased BDNF levels in adult sensory cortex does not re-open critical period plasticity (Galuske et al., 2000). Thus, it follows that the 5-aza induced reduction in BDNF expression may have contributed to the reversal of mature inhibitory synaptic features, and accordingly, the re-instatement of CP plasticity. Another developmentally regulated gene implicated in cortical maturation, REST, was also shown to increase its expression to the critical period level after 5'aza treatment. Studies have shown that developmental downregulation of REST expression is necessary for neurons to acquire mature characteristics (Ballas et al., 2005) and that transient upregulation of REST in adulthood facilitates a shift of neurons towards an immature state (Oh et al., 2018). Together, our results indicate that DNA-ME has a significant effect on the expression of genes that influence cortical maturation.

Although 5-aza treated animals showed a reduction in BDNF expression and increase in REST expression, the possibility remains that these effects are not a direct result from DNA demethylation. One intriguing possibility is that 5-aza treatment may be altering the expression of the multitude of methyl-binding proteins active in neurons. A study in Macaque monkeys showed that neurons in primary cortical areas and associative cortical areas have differing expression levels of methyl-binding proteins. Genes that are expressed in prefrontal cortex were enriched for methyl-binding protein 4 (MBD4) at promoters, while those same gene promoters were enriched for

MeCP2 in primary visual cortex (Hata et al., 2013). This indicates that while the methylation status of certain genes may be the same, their expression may be different due to the effects of different methyl-binding proteins. Finally, it is worth investigating how 5-aza treatment affects the expression of proteins that dictate neuronal fate. For example, during the CP, development of the parvalbumin-positive (PV+) interneuron (an important cell-type for CP plasticity), is tightly linked to the expression of homeoprotein, Otx2. Studies have shown that internalization of Otx2 by PV+ interneurons stimulates their functional maturation, and that the upregulation of Otx2 during the critical period is dependent on proper sensory experience (Sugiyama et al., 2008; Beurdeley et al., 2012; Bernard and Prochiantz, 2016; Sakai and Sugiyama, 2018). Furthermore, blocking PV+ internalization of Otx2 in adulthood re-establishes ocular dominance plasticity (Beurdeley et al., 2012). Therefore, the changes in gene expression seen in our 5-aza treated animals may be caused by an upstream effect on developmental transcription factors, such as Otx2.

In the present study, DNA-ME in the auditory cortex was significantly lower in CP than in adulthood. This is consistent with developmental upregulation of DNMT3a expression observed from PN Week 1 to Week 4 (Lister et al., 2013; Guo et al., 2014). Interestingly, blocking DNMT, which prevented upregulation of DNA-ME, prevented monocular deprivation-induced ocular dominance shift in visual CP (Tognini et al., 2015). Thus, it appears that while DNA demethylation reopens the critical period in adult cortex, normal critical period plasticity requires DNA-ME (Tognini et al., 2015; Apulei et al., 2019). It is possible that DNA-ME reduces plasticity to solidify experience-dependent circuit changes. Further studies tracking DNA-ME changes on developmentally regulated genes as the CP progresses may elucidate more information on the role of DNA-ME in regulating CP plasticity.

Figures

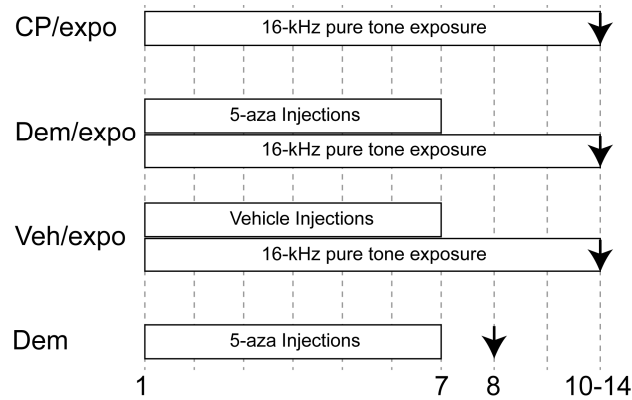


Figure 1. Timeline representation of 5-aza injection and sound exposure paradigm. Naïve animals (not shown) were taken directly from the colony with no exposure or injections. CP-expo animals began exposure on PN9, while the other adult groups were between 2 and 4 months of age during the treatment/exposure period.

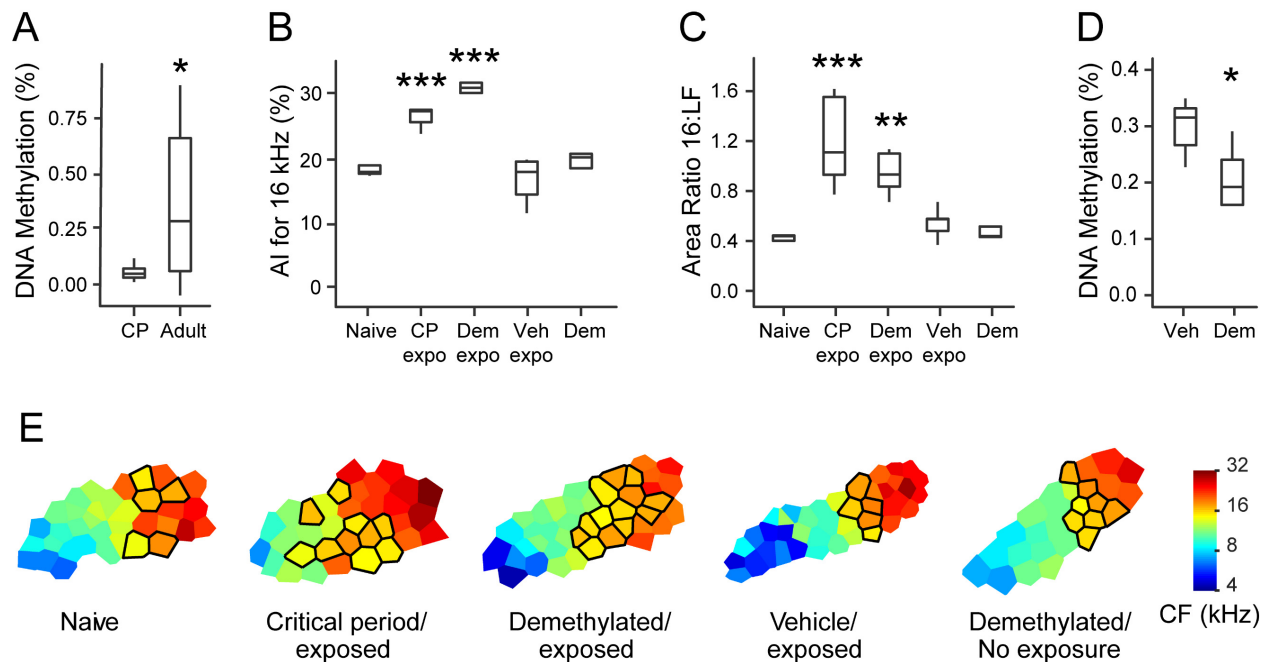


Figure 2. Pharmacological DNA demethylation re-establishes auditory critical period map plasticity in adult animals. **A)** Adult animals between 2-4 months of age and CP animals at P11 were sacrificed, and their brains harvested for methylation analysis. Methylation levels were found to be higher in adult auditory cortices ($n = 12$) than in the auditory cortices of CP animals ($n = 6$). **B)** Graph displaying the average area dedicated to sites within the exposure frequency. Both the critical period exposed and the demethylated exposed groups show a significant increase in the representation of 16 kHz ($n= 5$ for Naïve, CP-expo, Dem-expo and Veh-expo. $n=4$ for Dem). **C)** Graph displaying the ratio of the area of sites representing 16 kHz to a low frequency (8kHz-13.9kHz) The ratio was increased in the CP animals and demethylated exposed animals **D)** Graph displaying the difference in global methylation between the auditory cortices of vehicle exposed and demethylated animals. Vehicle treated mice had higher global methylation levels ($n = 8$) in the auditory cortex than mice treated with 5-aza ($n=4$). **E)** Example frequency maps of primary auditory cortex in five different groups of mice. Areas outlined in black indicate sites with CFs within the exposure frequency of 16 kHz (± 0.2 octaves). * $p < 0.05$, ** $p < 0.005$, *** $p < 0.0005$.

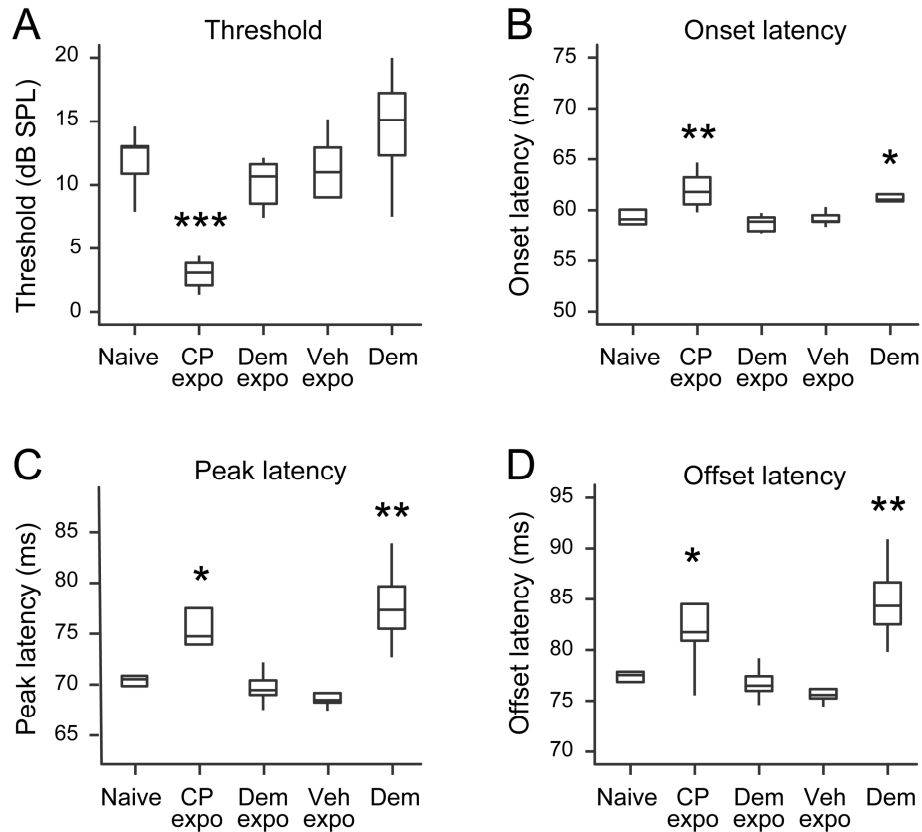


Figure 3. Pharmacological DNA demethylation in adults reverts some receptive field traits towards CP levels. **A)** A box and whisker plot showing the distribution of average thresholds for the five groups of mice (n= 5 for Naïve, CP-expo, Dem-expo and Veh-expo. n=4 for Dem). CP mice had a significantly lower threshold relative to the other groups. **B), C) and D),** show response onset, peak, and offset for the five groups. The CP and Dem groups had a prolonged response latency for each feature relative to the Naïve group. *p <0.05, **p<0.005, ***p<0.0005.

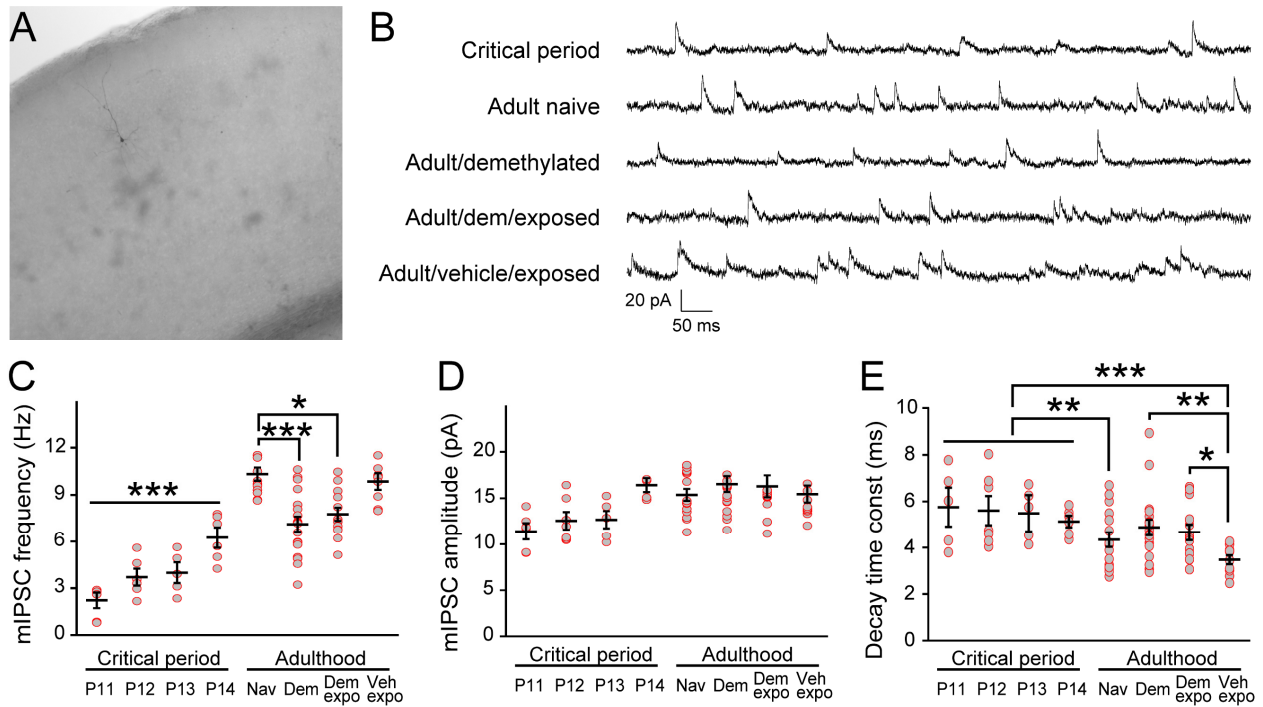


Figure 4. Pharmacological DNA demethylation reverts inhibitory synaptic function to an immature state. **A)** Image of biocytin stained pyramidal neuron within auditory cortex, used for patch clamp analysis. **B)** Representative current traces recorded from pyramidal neurons for the 5 groups tested: CP (n = 4 mice), adult Naïve (n = 4 mice), adult 5-aza treated with no exposure (Dem; n = 4 mice), adult 5-aza treated with exposure (Dem-expo; n = 4 mice) and adult vehicle treated with exposure (Veh-expo; n = 4 mice). **C)** Graph displaying the average mIPSC frequency for the 5 experimental groups. Both the Dem and Dem-expo groups had a significantly lower mIPSC frequency than Naïve adult animals, which is in line with the difference between CP animals and Naïve adult animals. **D)** Graph displaying the average mIPSC amplitude for the 5 experimental groups. No significant difference was found between any of the groups. **E)** Graph displaying the average mIPSC decay time constant. The Naïve and Veh-expo had a significantly lower average decay time constant compared to the CP group, which recapitulates previous reports.

Both the Dem and Dem-expo groups had a significantly higher mIPSC decay time constant compared to the Veh-expo group but did not have a significantly different mIPSC decay time constant compared to the CP group.

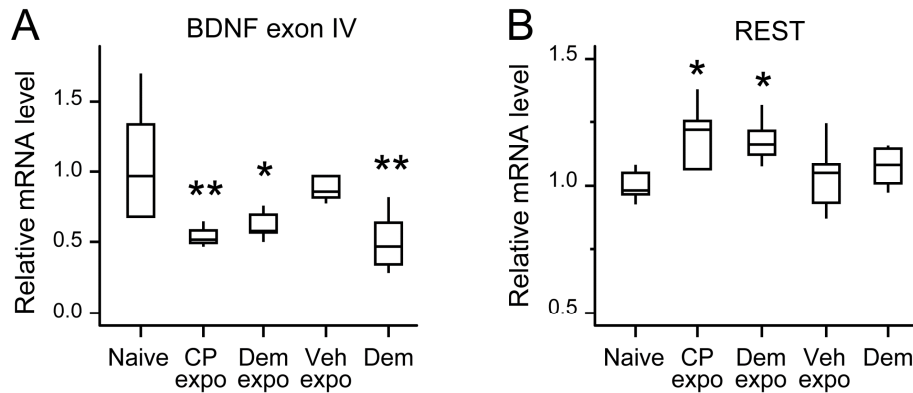


Figure 5. Pharmacological DNA demethylation reverses expression of developmentally regulated genes back to critical period levels. A) Relative BDNF mRNA expression level for the five experimental groups: CP (n = 5 mice), adult Naïve (n = 5 mice), Dem (n = 4 mice), Dem-expo (n = 5 mice) and Veh-expo (n = 4 mice). CP, Dem, and Dem-expo mice had significantly lower levels of BDNF expression relative to Naïve adult mice. **B)** Relative REST mRNA expression level for the five experimental groups: CP (n = 5 mice), adult Naïve (n = 5 mice), Dem (n = 4 mice), Dem-expo (n = 5 mice) and Veh-expo (n = 5 mice). Both CP mice and Dem-expo mice had significantly higher levels of REST compared to Naïve adult mice, while Dem mice were not significantly different from Naïve adult. *p < 0.05, **p < 0.005.

References

- Apulei J, Kim N, Testa D, Ribot J, Morizet D, Bernard C, Jourden L, Blugeon C, Di Nardo AA, Prochiantz A (2019) Non-cell Autonomous OTX2 Homeoprotein Regulates Visual Cortex Plasticity Through Gadd45b/g. *Cereb Cortex* 29:2384-2395.
- Ballas N, Grunseich C, Lu DD, Speh JC, Mandel G (2005) REST and its corepressors mediate plasticity of neuronal gene chromatin throughout neurogenesis. *Cell* 121:645-657.
- Baroncelli L, Scali M, Sansevero G, Olimpico F, Manno I, Costa M, Sale A (2016) Experience Affects Critical Period Plasticity in the Visual Cortex through an Epigenetic Regulation of Histone Post-Translational Modifications. *J Neurosci* 36:3430-3440.
- Bernard C, Prochiantz A (2016) Otx2-PNN Interaction to Regulate Cortical Plasticity. *Neural Plast* 2016:7931693.
- Beurdeley M, Spatazza J, Lee HH, Sugiyama S, Bernard C, Di Nardo AA, Hensch TK, Prochiantz A (2012) Otx2 binding to perineuronal nets persistently regulates plasticity in the mature visual cortex. *J Neurosci* 32:9429-9437.
- Bolton MM, Pittman AJ, Lo DC (2000) Brain-derived neurotrophic factor differentially regulates excitatory and inhibitory synaptic transmission in hippocampal cultures. *J Neurosci* 20:3221-3232.
- Chabot GG, Rivard GE, Momparler RL (1983) Plasma and cerebrospinal fluid pharmacokinetics of 5-Aza-2'-deoxycytidine in rabbits and dogs. *Cancer Res* 43:592-597.
- Dunning DD, Hoover CL, Soltesz I, Smith MA, O'Dowd DK (1999) GABA(A) receptor-mediated miniature postsynaptic currents and alpha-subunit expression in developing cortical neurons. *J Neurophysiol* 82:3286-3297.
- Fagiolini M, Hensch, T.K. (2000) Inhibitory threshold for critical-period activation in primary visual cortex. *Nature* 404:183-186.
- Galuske RA, Kim DS, Castren E, Singer W (2000) Differential effects of neurotrophins on ocular dominance plasticity in developing and adult cat visual cortex. *Eur J Neurosci* 12:3315-3330.
- Gervain J, Vines BW, Chen LM, Seo RJ, Hensch TK, Werker JF, Young AH (2013) Valproate reopens critical-period learning of absolute pitch. *Front Syst Neurosci* 7:102.
- Guo JU, Su Y, Shin JH, Shin J, Li H, Xie B, Zhong C, Hu S, Le T, Fan G, Zhu H, Chang Q, Gao Y, Ming GL, Song H (2014) Distribution, recognition and regulation of non-CpG methylation in the adult mammalian brain. *Nat Neurosci* 17:215-222.
- Hanover JL, Huang ZJ, Tonegawa S, Stryker MP (1999) Brain-derived neurotrophic factor overexpression induces precocious critical period in mouse visual cortex. *J Neurosci* 19:RC40.
- Hata K, Mizukami H, Sadakane O, Watakabe A, Ohtsuka M, Takaji M, Kinoshita M, Isa T, Ozawa K, Yamamori T (2013) DNA methylation and methyl-binding proteins control differential gene expression in distinct cortical areas of macaque monkey. *J Neurosci* 33:19704-19714.
- He LJ, Liu N, Cheng TL, Chen XJ, Li YD, Shu YS, Qiu ZL, Zhang XH (2014) Conditional deletion of *Mecp2* in parvalbumin-expressing GABAergic cells results in the absence of critical period plasticity. *Nat Commun* 5:5036.
- Hensch TK (2005) Critical period plasticity in local cortical circuits. *Nat Rev Neurosci* 6:877-888.

- Hensch TK, Fagiolini, M., Mataga, N., Stryker, M. P., Baekkeskov, S., Kash, S. F. (1998) Local GABA Circuit Control of Experience-Dependent Plasticity in Developing Visual Cortex. *Science* 282:1504-1508.
- Huang JZ, Kirkwood, A., Pizzorusso, T., Porciatti, V., Morales, B., Bear, M. F., Maffei, L., Tonegawa, S. (1999) BDNF regulates the maturation of inhibition and the critical period of plasticity in mouse visual cortex. *Cell* 98:739-755.
- Insanally MN, Albanna BF, Bao S (2010) Pulsed noise experience disrupts complex sound representations. *J Neurophysiol* 103:2611-2617.
- Itami C, Kimura F, Nakamura S (2007) Brain-derived neurotrophic factor regulates the maturation of layer 4 fast-spiking cells after the second postnatal week in the developing barrel cortex. *Journal of Neuroscience* 27:2241-2252.
- Katz LC, Crowley JC (2002) Development of cortical circuits: lessons from ocular dominance columns. *Nature Review Neuroscience* 3:34-42.
- Keuroghlian AS, Knudsen EI (2007) Adaptive auditory plasticity in developing and adult animals. *Progress in Neurobiology* 82:109-121.
- Kim H, Gibboni R, Kirkhart C, Bao S (2013) Impaired critical period plasticity in primary auditory cortex of fragile x model mice. *J Neurosci* 33:15686-15692.
- Lister R et al. (2013) Global epigenomic reconfiguration during mammalian brain development. *Science* 341:1237905.
- Lu Y, Christian K, Lu B (2008) BDNF: a key regulator for protein synthesis-dependent LTP and long-term memory? *Neurobiol Learn Mem* 89:312-323.
- Maffei L (2002) Plasticity in the visual system: role of neurotrophins and electrical activity. *Arch Ital Biol* 140:341-346.
- Majdan M, Shatz CJ (2006) Effects of visual experience on activity-dependent gene regulation in cortex. *Nature Neuroscience* 9:650-659.
- Martinowich K, Hattori D, Wu H, Fouse S, He F, Hu Y, Fan G, Sun YE (2003) DNA methylation-related chromatin remodeling in activity-dependent BDNF gene regulation. *Science* 302:890-893.
- Meadows JP, Guzman-Karlsson MC, Phillips S, Brown JA, Strange SK, Sweatt JD, Hablitz JJ (2016) Dynamic DNA methylation regulates neuronal intrinsic membrane excitability. *Sci Signal* 9:ra83.
- Meadows JP, Guzman-Karlsson MC, Phillips S, Holleman C, Posey JL, Day JJ, Hablitz JJ, Sweatt JD (2015) DNA methylation regulates neuronal glutamatergic synaptic scaling. *Sci Signal* 8:ra61.
- O'Leary DM, Ruff, N. L., Dyck, R. H. (1994) Development, critical period plasticity, and adult reorganizations of mammalian somatosensory systems. *Current Opinion in Neurobiology* 4:535-544.
- Oh YM, Mahar M, Ewan EE, Leahy KM, Zhao G, Cavalli V (2018) Epigenetic regulator UHRF1 inactivates REST and growth suppressor gene expression via DNA methylation to promote axon regeneration. *Proc Natl Acad Sci U S A* 115:E12417-E12426.
- Ohba S, Ikeda T, Ikegaya Y, Nishiyama N, Matsuki N, Yamada MK (2005) BDNF locally potentiates GABAergic presynaptic machineries: target-selective circuit inhibition. *Cereb Cortex* 15:291-298.

- Okaty BW, Miller MN, Sugino K, Hempel CM, Nelson SB (2009) Transcriptional and Electrophysiological Maturation of Neocortical Fast-Spiking GABAergic Interneurons. *Journal of Neuroscience* 29:7040-7052.
- Putignano E, Lonetti G, Cancedda L, Ratto G, Costa M, Maffei L, Pizzorusso T (2007) Developmental downregulation of histone posttranslational modifications regulates visual cortical plasticity. *Neuron* 53:747-759.
- Rodenas-Ruano A, Chavez AE, Cossio MJ, Castillo PE, Zukin RS (2012) REST-dependent epigenetic remodeling promotes the developmental switch in synaptic NMDA receptors. *Nat Neurosci* 15:1382-1390.
- Sakai A, Sugiyama S (2018) Experience-dependent transcriptional regulation in juvenile brain development. *Dev Growth Differ* 60:473-482.
- Sales AJ, Biojone C, Terceti MS, Guimaraes FS, Gomes MV, Joca SR (2011) Antidepressant-like effect induced by systemic and intra-hippocampal administration of DNA methylation inhibitors. *Br J Pharmacol* 164:1711-1721.
- Sugiyama S, Di Nardo AA, Aizawa S, Matsuo I, Volovitch M, Prochiantz A, Hensch TK (2008) Experience-dependent transfer of Otx2 homeoprotein into the visual cortex activates postnatal plasticity. *Cell* 134:508-520.
- Sweatt JD (2016) Dynamic DNA methylation controls glutamate receptor trafficking and synaptic scaling. *J Neurochem* 137:312-330.
- Tognini P, Napoli D, Tola J, Silingardi D, Della Ragione F, D'Esposito M, Pizzorusso T (2015) Experience-dependent DNA methylation regulates plasticity in the developing visual cortex. *Nat Neurosci* 18:956-958.
- Villers-Sidani E, Chang, E.F., Bao, S., Merzenich, M.M. (2007) Critical Period Window for Spectral Tuning Defined in the Primary Auditory Cortex (A1) in the Rat. *The Journal of Neuroscience* 27:180-189.
- West AE, Chen WG, Dalva MB, Dolmetsch RE, Kornhauser JM, Shaywitz AJ, Takasu MA, Tao X, Greenberg ME (2001) Calcium regulation of neuronal gene expression. *Proc Natl Acad Sci U S A* 98:11024-11031.
- Yu H, Su Y, Shin J, Zhong C, Guo JU, Weng YL, Gao F, Geschwind DH, Coppola G, Ming GL, Song H (2015) Tet3 regulates synaptic transmission and homeostatic plasticity via DNA oxidation and repair. *Nat Neurosci* 18:836-843.
- Zhang LI, Bao S, Merzenich MM (2001) Persistent and specific influences of early acoustic environments on primary auditory cortex. *Nat Neurosci* 4:1123-1130.
- Zhou C, Yan S, Qian S, Wang Z, Shi Z, Xiong Y, Zhou Y (2019) Atypical Response Properties of the Auditory Cortex of Awake MECP2-Overexpressing Mice. *Front Neurosci* 13:439.